AIAA JOURNAL
Vol. 49, No. 1, January 2011

Correlation of Flowfield and Acoustic Field Measurements in High-Speed Jets

Jérémy Veltin,* Benjamin J. Day,† and Dennis K. McLaughlin‡
Pennsylvania State University, University Park, Pennsylvania 16802

DOI: 10.2514/1.J050583

The present study demonstrates the capabilities of an optical deflectometry system to provide flowfield turbulence measurements that can be successfully correlated with acoustic field microphone measurements. Results from supersonic fully expanded jets are presented that document the coherence spectra between the flowfield and the acoustic field. The method is applied to jets with subsonic and supersonic convection speed, and shows a strong directionality of the emitted noise in both cases. Similar measurements performed in shock-containing jets with microphones in the forward arc reveal enhanced coherence at the dominant frequency of the broadband shock associated noise. Measurements were also performed with the optical sensors scanning radially outside of the jet in an attempt to obtain a measurement of the spectra in the acoustic near field. These results show an exponential decay of the signal magnitude characteristic of a region where hydrodynamic pressure fluctuations are dominant. The high level of skewness in these signals supports the concept that the crackle observed in the far field originates in the jet flowfield. Further radially, acoustic pressure fluctuations are successfully measured and correlated to the acoustic far field, thus demonstrating another application of this nonintrusive measurement technique in jet acoustics diagnostics.

I. Introduction

THIS paper strives to advance one of the main goals of the jet noise community: to provide experimental evidence to develop aeroacoustic theories for the accurate prediction of the noise radiated by jets. Jet noise is produced by the turbulence contained in a jet. Therefore, accurate knowledge of the turbulent properties is a fundamental ingredient in a noise prediction model. Improved understanding of these turbulent flow regions is something many investigators strive for.

Velocity, pressure and density fluctuations within jets have been measured in a number of past experimental works. The purpose of these measurements is to gain knowledge of the main parameters of the noise generation process: the length scales and the growth and decay rates of the turbulent structures. The initial turbulence measurements designed to learn something of jet turbulence responsible for noise production were all conducted with hot-wire anemometry in relatively low speed subsonic jets; e.g. Davies et al. [1], Bradshaw et al. [2], and Crow and Champagne [3] to name just a few. Together with more recent data of this kind, such as those provided by Morris and Zaman [4], a very good database exists, describing the turbulent properties of subsonic jets.

Supersonic measurements of the jet turbulence are more challenging. Early supersonic turbulence measurements were performed by McLaughlin et al. [5] and Troutt and McLaughlin [6], who were able to use hot-wires extensively in supersonic jets by conducting the experiments in a reduced density anechoic chamber. Supersonic measurements can also be obtained using laser Doppler velocimetry (LDV), however, the technique relies on particle seeding of the flow, which raises issues such as nonuniform seeding and inertial "slippage" of the particles. Additionally, most LDV systems do not produce signals that are continuous in time. In spite of these difficulties, very good data were obtained with laser velocimetry by Lau [7] and more recently by Kerhervé et al. [8]. Particle image velocimetry (PIV) measurements have also recently been used extensively for this purpose by Bridges [9] and by Kastner et al. [10]. While spatial resolution is excellent for this technique, sufficient time resolution remains difficult to obtain to allow extensive time accurate two point space-time correlations in supersonic jets. Fully nonintrusive measurements were also made using a molecular Rayleigh scattering technique, most recently by Panda and Seasholtz [11], and Panda et al. [12]. The technique possesses excellent capabilities, but is very difficult to set up and calibrate and time consuming to use. Few researchers have invested in the infrastructure to develop the PIV, LDV or Rayleigh scattering systems applied to supersonic jet flows.

More recently, optical deflectometry (OD) has been used in the Pennsylvania State University (PSU) jet noise laboratory to measure the turbulence properties of supersonic jets. The main type of measurement one can obtain from an OD system is a simple correlation of the time signals with different axial separation distance Δx between the two optical sensors. The OD setup produces two point correlation measurements with very high frequency response and ease of setup. However, the nature of the system makes it difficult to obtain specific values for the density or density gradient, such that precise calibration of the system in order to obtain a direct measurement of the density remains to be developed. Another limitation of the OD system was uncovered by Doty and McLaughlin [13] who underlined the difficulties of obtaining meaningful measurements in hot and heat-simulated jets. Therefore, this study focuses solely on cold, pure air jets.

While two point space-time correlations of the turbulence properties have been investigated in detail in past studies, such as Doty and McLaughlin [13] and Harper-Bourne and Fisher [14], the present work focuses on direct correlation between the turbulence properties of the flow and far-field microphone measurements. Such an approach was used by a few researchers in the past, including Seiner and Reethof [15], who used hot-wires in the flow, or Schaffar [16], using LDV. However, as discussed by these authors, most resulting correlations demonstrated that 1) there is significant noise produced by the presence of the hot-wire probes in the flow and 2) uncertainties in the LDV measurements cast some doubt on those results obtained. More recently, Rayleigh scattering technique in

Presented as Paper 2009-3250 at the 15th AIAA/CEAS Aeroacoustics Conference , Miami, FL, 11–13 May 2009; received 30 March 2010; revision received 7 August 2010; accepted for publication 17 October 2010.

*Postdoctoral Fellow, Department of Aerospace Engineering. Student Member AIAA.

†Graduate Research Assistant, Department of Aerospace Engineering. Student Member AIAA.

‡Professor, Department of Aerospace Engineering. Fellow AIAA.

conjunction with microphone measurements were obtained by Panda and Seasholtz [11], and Panda et al. [12], providing reliable correlation measurements between the flowfield and the acoustic far field. To some extent, the current study presents results using the OD technique that are similar to those obtained by Panda et al. [12] with the Rayleigh scattering technique.

The goal of the current study is to demonstrate the capability of the OD technique to provide measurements in the jet flowfield that are directly correlated to microphone measurements in the acoustic far field. By developing an improved understanding of the coherence properties of the far-field noise with turbulence in the flowfield, a longer range goal is to develop more accurate computational models of the noise generation. The cross-correlation coefficient as well as the coherence were measured for supersonic jets of different speeds. Shock-free as well as shock-containing jets were explored, with microphones in the forward and the rear arc in an attempt to capture both the dominant noise radiation and the broadband shock associated noise (BBSAN). Similar experiments with the optical sensors in the acoustic near field are also presented, showing that detection of the highest amplitude sound is possible with the OD technique; very strong correlation between the near and the far acoustic fields was obtained. While this study only shows point to point correlations, more advanced processing of similar data is underway by Papamoschou et al. [17], using a phased array in the acoustic far field correlating with simultaneous OD flow measurements.

II. Experimental Facilities, Setup, and Procedure

A. Facilities Description

Part of the experiments presented in this study were conducted in the PSU high-speed jet noise facility, shown in Fig. 1. High pressure air, pressurized to 1.34 MPa (195 psig) by a CS-121 compressor combined with a KAD-370 air dryer both manufactured by Kaeser Compressors, is provided from two 18.9 m^3 tanks. The air flow is then regulated via pressure regulators and control valves located in a piping cabinet before being fed to a plenum that has a number of turbulence management elements upstream of a lengthy settling chamber. Following this settling chamber, the air is exhausted through a nozzle into the anechoic chamber. A pitot probe is embedded in the middle section of the plenum to provide, via a pressure transducer, the total pressure upstream of the nozzle. The anechoic chamber walls are covered with fiberglass wedges and have an approximate cutoff frequency of 250 Hz. An exhaust collector and fan on the opposite wall of the plenum in the anechoic chamber prevents flow circulation and possible pressure buildup. More detailed descriptions of the facility can be found in Doty and McLaughlin [18] and in McLaughlin et al. [19].

The acoustic measurements at PSU were performed using four microphones, arranged so that the plane of the microphone diaphragms is positioned on the axis of the jet (grazing incidence). The microphones used are 1/8 in. pressure-field microphones, type 4138 from Brüel and Kjaer (B&K), and type 40DP from GRAS. The microphone calibrations are performed with a B&K acoustic calibrator, model 4231, and the microphone calibration constants are recorded to provide the conversion from the measured voltages to the equivalent pressure. The analog time-domain signals from the microphones are routed through a Nexus, B&K signal conditioner or a GRAS model 12AN power module and then amplified and filtered for anti-aliasing thus enabling their accurate digital conversion in the following acquisition. Acoustic measurements at PSU are typically performed on a radius of between 100 and 140 jet diameters from the nozzle exit, depending on nozzle diameter [19]. However in this study the microphones were positioned so they would be at the same azimuthal location as the OD sensor. For this reason, different microphone supports were manufactured, and located in the vertical plane of the jet, and consequently the microphone range was limited to 40 to 50 jet diameters.

Both the acoustic signals and the signals from the optical sensors are routed through high-pass filters set to 500 Hz, removing any undesirable low frequency noise that could contaminate the data. A PCI-6123 National Instruments DAQ board acquires the time-domain data which are then stored in binary files that are passed to the following stage for processing and correction. An acquisition frequency of 300 kHz is sufficient for fine resolution in frequency and adequate for statistical significance of the final quantities. However, in order to obtain a finer resolution in retarded time when calculating the cross-correlation coefficients, an acquisition rate of 500 kHz was used. Once the time data are acquired with a LabVIEW controlled personal computer, the binary files are read and processed using Matlab.

Additional experiments were conducted in the University of California, Irvine (UCI) jet noise facility using the same optical deflectometer system. The facility layout at UCI is very similar to the PSU facility and detailed descriptions of both the facility and the specifics of the acquisition setup can be found in Papamoschou et al. [17].

Three nozzles were used for the measurements presented in this study. Two stainless steel 12.7 mm (0.5 in.) diameter nozzles were used for the experiments performed at PSU, with respective design Mach number $M_d = 1.0$ and 1.5. The experiments performed at UCI were conducted with a 12.7 mm (0.5 in.) diameter nozzle with a design Mach number $M_d = 1.75$. The two supersonic nozzles were contoured converging-diverging nozzles designed by the method of characteristics to produce parallel, shock-free flow at the exit when operated at perfectly expanded pressure ratios.

B. OD Setup

An optical deflectometer is an instrument derived from the Schlieren principle, which allows simultaneous measurements at a few spatial locations. The measured signals are proportional to the

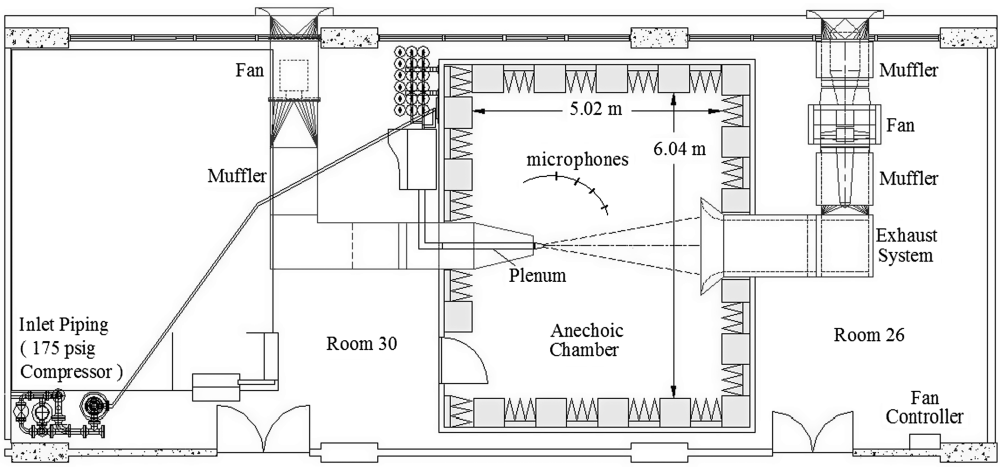

Fig. 1 The PSU high-speed jet noise facility.

light intensity at a specified point on the Schlieren image plane. The fluctuation of light intensity is caused by density gradient fluctuations within the test section as the deflection of the light moves the beam into and out of the (horizontally oriented) knife edge. A new OD setup was designed for these experiments, to be used at the PSU and at the UCI. The layout of this new system can be seen in Fig. 2. The basic design of this new system is in many ways very similar to the one described in Doty and McLaughlin [13] and extensively used in previous studies at PSU. Building on past experience, attention was paid to refining the design, such as maximizing the amount of light captured from the light source to produce the parallel beam. The whole system was dimensioned to fit in the UCI small scale jet noise laboratory and to be easily shipped there. However, during the design process, two major differences (upgrades) were incorporated into this new design:

1) The new design included four individual photo sensors, instead of the two sensors used in the PSU system. To do so, the two photomultiplier tubes were replaced by much smaller avalanche photodiodes (APDs), Hamamatsu model C5460-01. The APDs were placed in (two) pairs on the two image planes. One pair was mounted on orthogonal manual traverses while the second pair was fitted onto motorized traverses and piloted through a computerized controller. This provided the capability of making measurements faster and having two fixed reference points when performing cross-correlations.

2) The second upgrade aimed at altering the optics arrangement so that the nozzle itself is accurately focused at the image planes of the receiving optics. This resulted in increased fidelity of the Schlieren images. It is noted that the four sensor OD system facilitated processing all four signals using a delay and sum algorithm to provide additional interpretive data of the jet turbulence (as reported by Papamoschou et al. [17]).

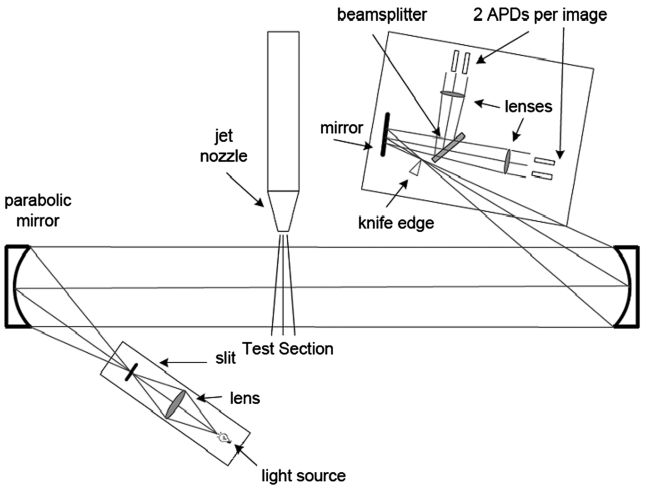

Fig. 2 Schematic of new OD setup.

The voltages measured from the OD sensors relate to fluctuations in light intensity, which relate to fluctuations of density gradients in the flow. It is not practically possible to determine the exact relationship between the specific density gradient within the sensing volume of the OD and the photo detector output voltage. Additional difficulty arises because the OD signals are produced from an integration of effects throughout the entire light path. Finally, due to the presence of the horizontal knife edge in the OD setup and the fact that the density gradient in a Cartesian coordinate changes sign from one side of the jet to another, one shear layer appears to be light while the other is dark. The experiments presented here were all performed in the light shear layer and focus on cross-correlation coefficients and coherence of the OD signals with respect to the acoustic signals. Most of the data are presented in nondimensional form.

Validation measurements were performed in order to ensure that the new OD system produces reliable results. As an example of these validation measurements, Fig. 3 presents the cross-correlation coefficients between two OD sensors at various axial separations located in the shear layer of a Mach 0.9 jet. As can be seen, the results from the current setup are nearly identical to the setup used by Doty and McLaughlin [13], with only very small differences in the magnitude and location of the peaks. Moreover, despite the difficulties in interpreting the quantity being measured by the OD signals, the data are consistent with hot-wire correlation coefficients measured by Davies et al. [1] in a lower speed jet ($M_j = 0.45$). The envelope of the correlation coefficient curves represents the moving frame autocorrelation function where the dominant turbulent scales are moving at an average convection velocity U_c. Since the time axis is nondimensionalized, it is expected to obtain matching envelopes between subsonic jets of different speeds. More comparisons of this type were performed by Doty and McLaughlin [13]. Finally, repeatability of the measurements was demonstrated by performing the same measurements following a few-week interval, with different atmospheric conditions, and verifying that the resulting correllelograms matched properly.

C. Data Processing

Time signals from each individual OD sensor and microphone represent different measured properties, but some of the data processing of these signals is the same. Defining $p_i(t)$ to be the voltage signal of the ith sensor (either a microphone or an OD sensor), statistical quantities can be examined such as the mean μ_i, the variance σ_i and the skewness sk_i. Then, postprocessing can be

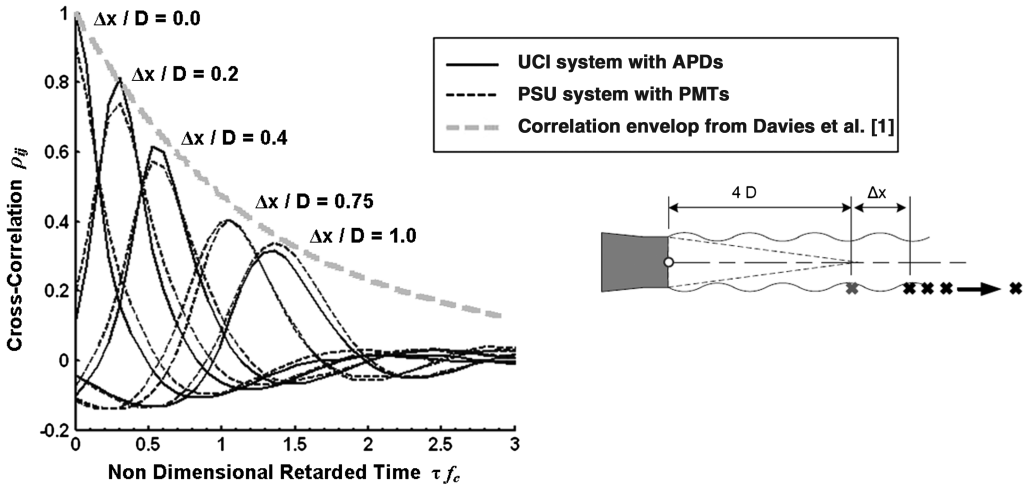

Fig. 3 Cross-correlation coefficient function between OD sensors at various axial separations for a jet issuing from a converging nozzle at $M_j = 0.9$, and envelop of cross-correlation coefficient curves between hot-wire probes in a $M_j = 0.45$.

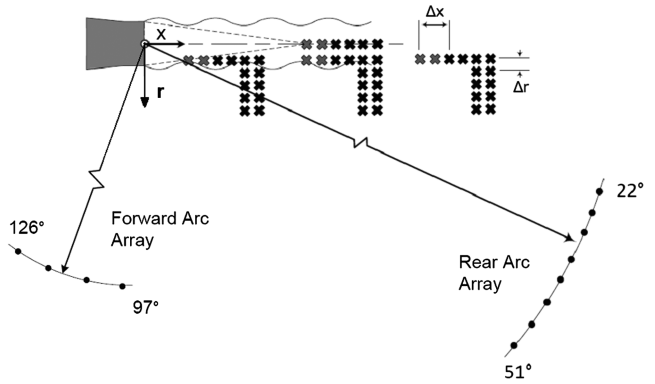

Fig. 4 Setup showing microphone arrays located in the rear and forward arc as well as several sample locations for the OD sensors.

performed, where the time data are typically split into 4096 point windows in order to obtain a fine resolution in frequency. A Hanning window function is applied and 50% overlap is used between each window, resulting in a total of 199 windows. The fast Fourier transform is calculated on each window and then averaged, yielding the double sided power spectral density $S_{ii}(f)$. If the signal from a second sensor $p_j(t)$ is acquired simultaneously, then its spectral density $S_{jj}(f)$ can be determined as well as the cross spectral density $S_{ij}(f)$ of the two signals. From these, the single sided power spectral densities $G_{ii}(f)$ and $G_{jj}(f)$, and the cross spectral density $G_{ij}(f)$ can easily be computed. The auto and cross-correlation functions, respectively $R_{ii}(\tau)$, $R_{jj}(\tau)$ and $R_{ij}(\tau)$, can then be calculated by taking the inverse Fourier transform of the spectral densities. Additionally, the auto and cross-correlation functions also relate to the time signal by a convolution, as shown in Eq. (1):

$$R_{ij}(\tau) = \frac{1}{T}\int_0^T p_i(t)\,p_j(\tau + t)\,\mathrm{d}t \tag{1}$$

In this formula, T represents the time of a sample window and τ is the time delay (or retarded time). Typically, the time delay is nondimensionalized by multiplying it by the characteristic frequency f_c of the jet flow. Additionally the cross-correlation coefficient function can be calculated for two signals, and consists of a normalization of the cross-correlation function, as defined in Eq. (2):

$$\rho_{ij}(\tau) = \frac{R_{ij}(\tau)}{(R_{ii}(0).R_{jj}(0))^{1/2}} \tag{2}$$

Finally, the coherence γ_{ij} between two signals is computed from G_{ii}, G_{jj} and G_{ij} following the formula in Eq. (3):

$$\gamma_{ij}^2(f) = \frac{|G_{ij}(f)|^2}{|G_{ii}(f)|.|G_{jj}(f)|} \tag{3}$$

D. Experimental Conditions

A number of measurements were made with the preceding setup, both in the PSU and in the UCI jet noise facilities. In these experiments, simultaneous acoustic measurements in the far-field and flowfield optical signals were acquired with the goal of correlating the two types of signals. Experiments at PSU focused on both shock-containing and fully expanded jets, with four microphones used successively in the forward and rear polar arcs at a distance of 40 and 50 nozzle diameters, respectively, as measured from the jet centerline with the origin at the center of the nozzle exit. The experiments conducted at UCI focused primarily on fully expanded jets, and on the simultaneous use of a phased microphone array (with beamforming data processing), as reported by Papamoschou et al. [17]. Eight microphones were used for these measurements, arranged on a polar array at approximately 80 nozzle diameters from the nozzle exit and with their diaphragms facing the jet exit (normal incidence). The results presented in this study consist of correlation measurements between a single OD signal with a single microphone, with each sensor positioned at widely varying locations. A diagram summarizing the microphone array locations and typical OD measurement locations is shown in Fig. 4.

OD measurements in both facilities were made in both the middle of the light shear layer and the centerline of the jet. However, measurements on the centerline are less precise, since the light must pass through a rather thick region of density fluctuations and the integrative effects over this thick region are significant. Measurements in the shear layer, however, are less affected by this integration effect as the light passes through a thinner region at the edge of the jet. The optical measurements conducted at PSU were performed with a small number of spatial locations for the OD sensors and varying jet conditions, while the measurements performed at UCI concentrated on fewer jet conditions with more thorough flow measurements, at varying locations. Typically, one pair of optical sensors was positioned at a specified location and left fixed, while the second pair scanned axially or radially through the jet. This procedure was repeated for several axial stations in the jet, as represented in Fig. 4, with one pair of fixed OD sensors and the second pair moving through axial steps Δx or radial steps Δr.

The jet operating conditions for experiments at both facilities are summarized in Table 1. The experiments were conducted using cold pure air jets only. The design Mach number of a given nozzle is noted as M_d, while M_j corresponds to the Mach number of the fully expanded jet plume. The convective Mach numbers M_c presented in this table were computed from measurements of the average convection velocity U_c via measurements of the cross-correlation coefficient between optical sensors within the shear layer ($r/D = 0.5$) and $4D$ downstream of the jet exit plane. While this convection velocity will evolve along the jet [7], this measurement is representative of the convection speed of the dominant turbulent structures within the jets.

For the fully expanded $M_j = 1.75$ case, it should be noted that the average convection speed is supersonic. Therefore, the jet produces Mach waves that radiate to the far field. The propagation angle of these waves (relative to the jet centerline and using the average convective Mach number $M_c = 1.14$) can be calculated to be

$$\theta = 90 - \sin^{-1}\left(\frac{1}{M_c}\right) \approx 28.7^\circ \tag{4}$$

Moreover, it was shown by Troutt and McLaughlin [6], Harper-Bourne [20], Kerhervé et al. [21] and Morris and Zaman [4] that the convection velocity varies logarithmically with frequency. The same

Table 1 Jet operating conditions

M_d	M_j	U_j (m/s)	Reynolds number	M_a [a]	f_c [b](kHz)	M_c	Facility	Figures	Microphone locations	Peak OASPL [c]
1.5	1.5	428	710,000	1.26	33.6	0.96	PSU	7, 9, 10	Rear arc	127 dB
1.75	1.75	473	1,061,000	1.39	37.2	1.13	UCI	6, 8, 11, 12, 13, 14, 15, 16	Rear arc	130 dB
1.0	1.5	428	770,000	1.26	31.0	0.95	PSU	17	Forward arc	127 dB
1.0	1.8	479	1,197,000	1.41	31.6	1.15	PSU	18	Forward arc	131 dB
1.5	1.8	479	1,102,000	1.41	34.2	1.14	PSU	18	Forward arc	131 dB

[a]Acoustic Mach number $M_a = U_j/a_\infty$, where a_∞ is the ambient speed of sound.
[b]Characteristic frequency of the jet $f_c = U_j/D_j$, where D_j is the equivalent diameter of the fully expanded plume.
[c]All values correspond to lossless OASPL propagated to $80D$.

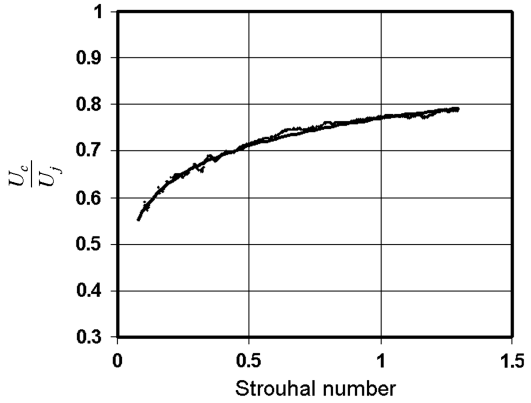

Fig. 5 Measured convection velocity as a function of Strouhal Number, *St*, for a $M_d = M_j = 1.5$ jet.

observation can be made from the present measurements, as shown in Fig. 5 for the fully expanded $M_j = 1.5$ jet. This convection velocity is computed from the derivative of the phase of the cross-spectra between two OD signals with respect to separation distance. This variation of U_c with f demonstrates that even for a jet condition for which the average convection velocity is subsonic, often the highest frequency components travel at supersonic speeds, hence radiating noise with similar characteristics to classical Mach wave radiation. These high frequency Mach waves are often most visible in Schlieren visualizations which are more pronounced at the short wavelengths (and high frequencies).

III. Results and Discussions

The first part of the results will focus on correlation between optical sensors scanning the jet flow and microphone far-field measurements in the rear polar arc. The experimental data acquired for this part were gathered both at the PSU and the UCI facilities and with fully expanded supersonic jets.

The second set of results presents measurements performed in the very near field of the jet, and their subsequent correlation with far-field acoustic measurements in the rear arc. While a small number of measurements of this kind were performed at PSU, those presented here were acquired at UCI. Once again, the focus is on fully expanded jets.

Finally, the third part presents measurements performed at PSU with shock-containing jets and shows significant correlation between the flowfield optical signal and the far-field microphone signals in the forward arc of the plane.

A. OD Sensors in the Jet Correlated to Rear Arc Microphones

The rms value of the OD sensor signals can first be examined in order to try and visualize the parts of the flow with high density fluctuations. This in turn gives a measurement of the amount of turbulence in the jet for different locations. The OD sensor rms voltage output is plotted along the lipline and the centerline of a fully expanded $M_j = 1.75$ jet and presented in Fig. 6. It is important to recall that the output from the OD sensors is expressed in voltage. While these voltage values can be directly related to light intensity and therefore to dimensional flow quantities such as density gradients, a reliable calibration technique has yet to be developed. Words of caution should also be expressed when examining OD signals along the centerline of the jet as the sensing volume traverses the whole jet and the resulting signal corresponds to an integration along this volume. The time mean density gradients in the mixing layers are mainly in the radial direction. When the light beam intersecting the jet centerline is interrogated, it is exposed to (time mean) density gradients with little preferential direction. This light beam relies largely on large scale jet flapping to produce cross beam density gradients. Because the knife edge is oriented horizontally, the cross stream gradients are the ones that dominate the OD time varying signal. The signal strength shown in Fig. 6 reaches a peak at about $x/D = 9$ on the lipline, while on the centerline, this maximum occurs at around $x/D = 13$. This observation is consistent with noise source measurements made by Laufer et al. [22] using a spherical reflecting microphone system for noise source location measurements of $M_j = 1.47$ and 1.97 jets. Therefore, one would expect the noise generation at the centerline and the lipline to reach peaks at these same locations.

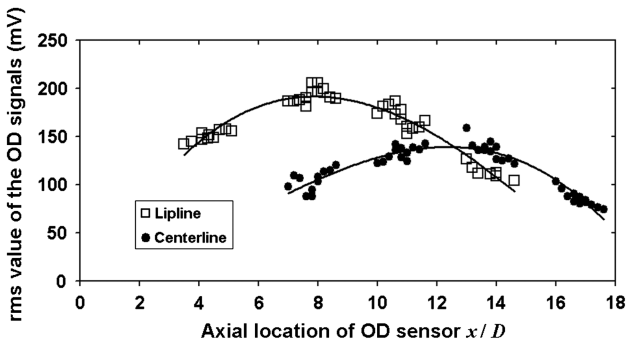

Fig. 6 RMS values of the OD signals along the axial direction in a fully expanded, $M_j = 1.75$ jet.

Another observation that can be made from this plot is that the maximum rms value of the signal measured on the lipline of the jet is noticeably higher than the maximum value of the signal measured on the centerline. On the other hand, when the rms of the OD signal measured along the centerline reaches its maximum, it is higher than on the lipline at the corresponding location. Therefore, one would expect the centroid of the noise generation location to progressively switch from the lipline to the centerline between $x/D = 9$ and $x/D = 13$.

A comparison can be made between the output spectra from the optical sensors at different locations within the fully expanded $M_j = 1.5$ jet and similar measurements performed using other techniques. Figure 7 presents the power spectral density of the current optical measurements for different downstream locations along the lipline (Fig. 7a), similar measurements performed in a $M_j = 1.8$ jet using the Rayleigh scattering technique (Panda and Seasholtz [11], Fig. 7b), with LDV in a $M_j = 1.2$ jet (Kerhervé et al. [8], Fig. 7c), and with wedge hot-film probe in a $M_j = 2.0$ jet (Seiner et al. [23], Fig. 7d). The nature of the measurements is different since some of these techniques provide a measurements of the magnitude of the velocity or mass velocity fluctuations (LDV, hot-film) while others relate to density fluctuations (OD, Rayleigh scattering). The general trend is nevertheless the same for all techniques, with low frequency spectral components growing with increasing downstream position consistent with the larger turbulent scale size downstream. A more direct comparison can be made at one downstream location, $x/D = 6$, on the nozzle lipline, by normalizing spectra from all measurement methods with their respective mean square values (the area under the PSD curves). These data, plotted in Fig. 8, show the close agreement between all spectra measured in jets of Mach number between 1.5 and 2.0, even though the measurements are made with three entirely different instruments. Additional data presented in the MS thesis of Day [24] show that the velocity spectra of Kerhervé et al. [8] (performed in a cold $M_j = 1.2$ jet) match very closely to recent hot-wire measurements of Morris and Zaman [4] in a low subsonic round jet. All these comparisons provide additional confidence in the ability of the optical deflectometer to make meaningful turbulence measurements in supersonic jets.

As a first try of flowfield measurement correlations with far-field acoustic signals, correlation was performed between an optical sensor located at 4 diameters downstream in the mixing layer of a fully expanded $M_j = 1.5$ jet and microphones on a polar array in the forward polar arc ($\theta < 90°$). The computed cross-correlation coefficient functions are shown in Fig. 9. Significant peaks of correlation are obtained, demonstrating a direct relation between the flowfield and the acoustic far field. Similar results were obtained with the optical sensor positioned at different downstream locations and

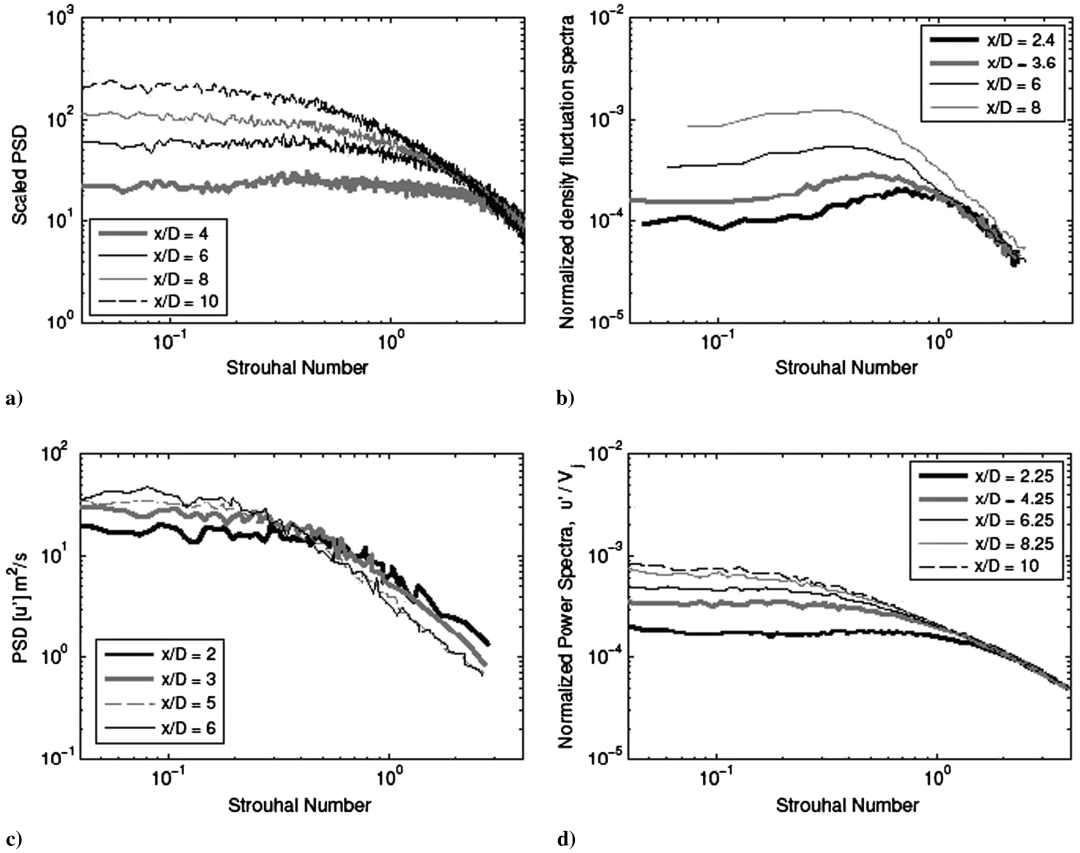

Fig. 7 Power spectra at different axial locations in fully expanded jets, obtained through different techniques: a) $M_j = 1.5$, OD present study, b) $M_j = 1.8$, Rayleigh scattering [11], c) $M_j = 1.2$, LDV [8], and d) $M_j = 2.0$, hot-film [22].

jets running at different speeds. The maximum peak of the correlation coefficient found in this configuration of the setup is approximately 0.1. This is similar in magnitude to the amount of correlation measured by Panda and Seasholtz [11] between the local jet density and the sound pressure fluctuation using the Rayleigh scattering technique along the centerline of a $M_j = 1.4$ jet. It also shows a strong dependence on the polar location of the microphones: while the magnitude of the peak of the correlation coefficient function is maximal for $\theta = 22°$, it drops with increasing polar angle to completely disappear for $\theta = 41°$. It is quite interesting that there is such a noticeable difference between these correlations across such a small range of polar angles (as little as 10° around the 30° location) and tends to demonstrate a strong directionality of the noise components that correlates with the flowfield optical measurements. The measurements are, however, too close to the jet exit plane and do not cover adequately enough the lower polar angle range, to be able to accurately determine the peak noise emission direction. Finally, it should be mentioned, as first pointed out by Panda and Seasholtz [11], that the correlation peak occurs at non dimensional retarded time values around $\tau.f_c = 63$, which directly relates to the distance from the optical sensor to the microphones via the ambient sound speed ($a_\infty = 343$ m.s^{-1}) as follows:

$$\tau = \frac{R}{a_\infty} \tag{5}$$

The slight differences in the retarded time value obtained from the correlation with each microphone can be directly related to small differences in their physical distance relative to the optical sensor focusing point.

The peak magnitude of the cross-correlation coefficient function ρ_{ij} can then be plotted for different locations of the optical sensor and all available polar angles, as shown in Fig. 10a for the fully expanded $M_j = 1.5$ jet. There is a significant change in the correlation peak with increasing downstream position of the optical sensor, up to a distance of 5 diameters downstream. This tends to point to this location as the main noise generation location, but measurements further downstream are clearly needed. It is noted that the magnitude of the correlation is highest for the lowest polar angles, and almost entirely disappears for the largest polar angle value (41°), results that are consistent with the observation of Fig. 9.

A very similar experiment was performed in the UCI facility, but this time with the fully expanded $M_j = 1.75$ jet. These OD measurements produced the rms values presented earlier in Fig. 6.

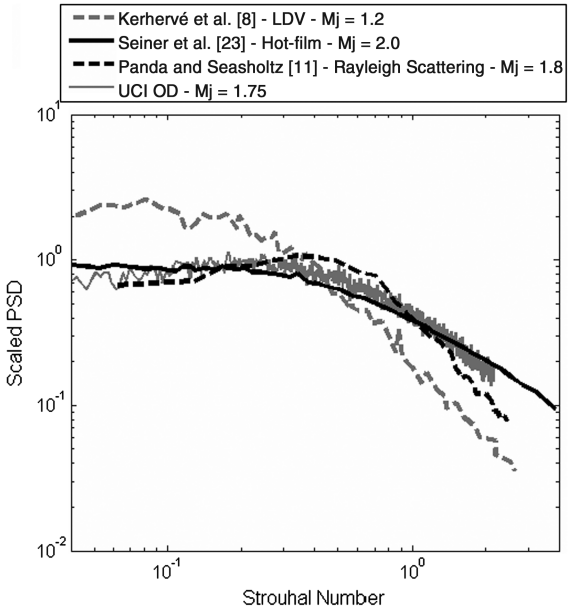

Fig. 8 Normalized power spectra at $x/D = 6$ and in fully expanded jets, obtained through different techniques.

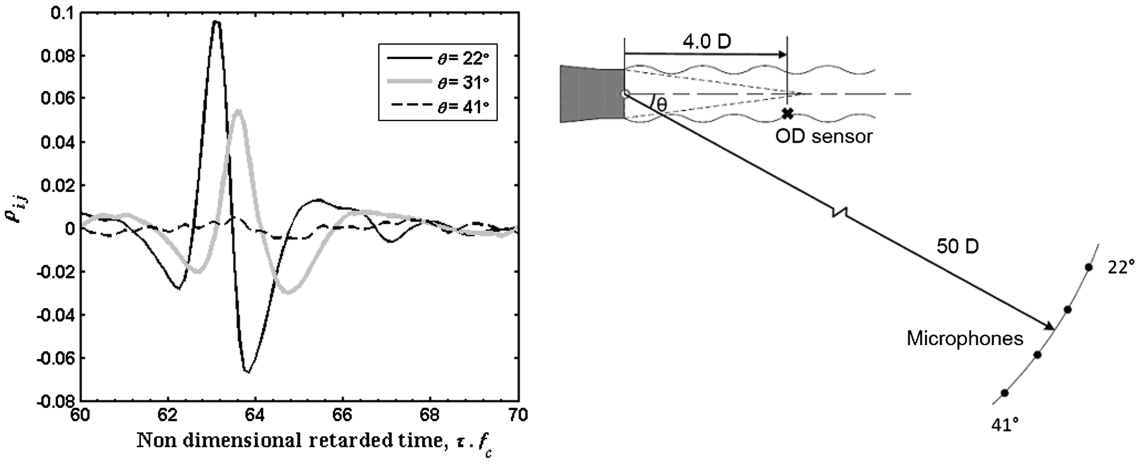

Fig. 9 Correlations between an OD sensor at the lipline and $x/D = 4.0$ and microphones in the rear arc for $M_d = 1.5$, $M_j = 1.5$.

The resulting peak magnitudes of ρ_{ij} are plotted in Fig. 10b for different downstream locations of the OD sensor and microphone polar angles ranging from $\theta = 22$ to 51°. Once again, the correlation is the highest for downstream location around $5D$ and drops dramatically further downstream, showing consistency with the $M_j = 1.5$ jet data of Fig. 10a. The amount of correlation also drops drastically for the highest values of θ and seems to be maximum for $\theta = 28°$. For a downstream distance of roughly $5D$, the relative angle between the OD sensor and the far-field microphone (located at $\theta = 28°$ and a nondimensionalized distance $R/D = 80$) can be computed as follows:

$$\theta_r = \tan^{-1}(80.\sin(28°)/80.\cos(28°) - 5) = 29.8° \qquad (6)$$

This agrees quite closely with the prediction of the Mach wave radiation angle computed from the convection velocity in Eq. (4) that lead to a polar angle $\theta = 28.7°$. At this point it is noted that there is very little difference between the levels of correlation between the $M_j = 1.5$ and $M_j = 1.75$ jets aside from the polar angle at which the OD to microphone correlations maximize. This is so in spite of the fact that the $M_j = 1.75$ jet produces Mach wave radiation and the $M_j = 1.5$ jet with its subsonic convection velocity presumably does not since the dominant turbulent structures convect subsonically.

To gain some knowledge of the frequency content that correlates between the flowfield measurements and the acoustic far field for the $M_j = 1.75$ jet, the coherence is plotted between the OD sensor within the mixing layer and a microphone fixed near the Mach wave

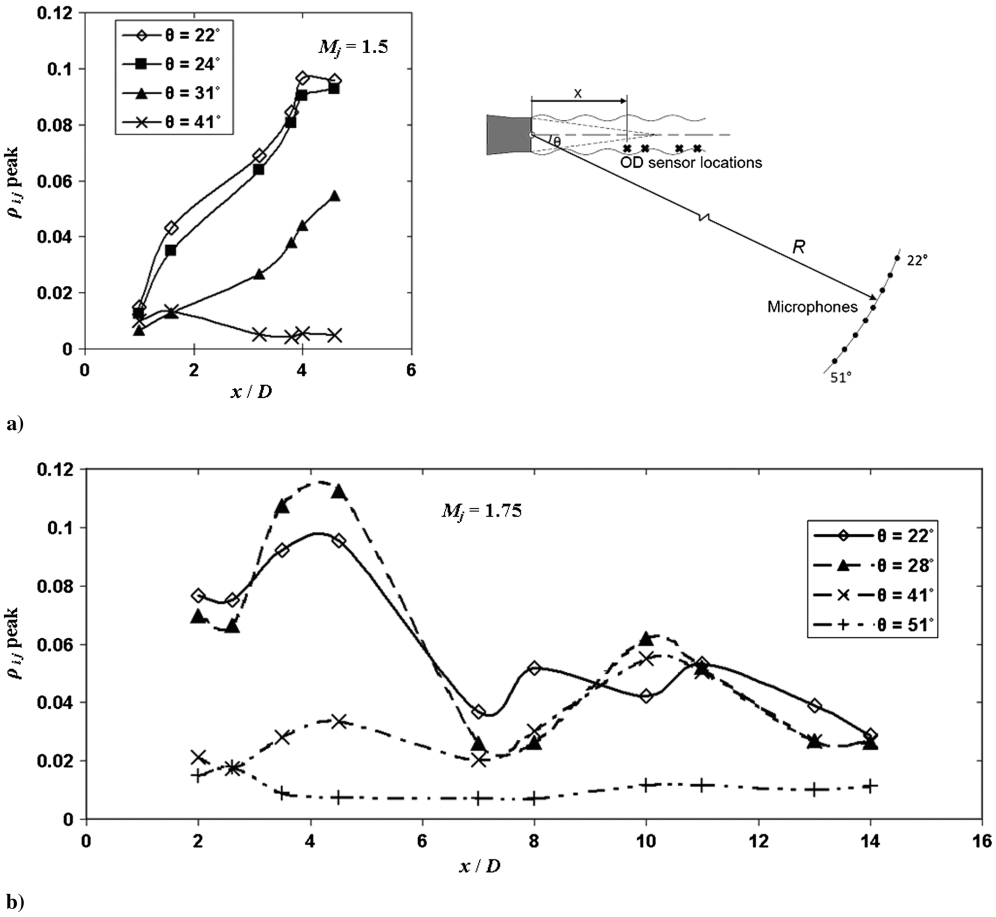

Fig. 10 Peak correlation between OD sensor and microphone in the rear arc with OD sensor at various axial locations along the lip line of a fully expanded jet: a) $M_j = 1.5$, $R/D = 50$ and b) $M_j = 1.75$, $R/D = 80$.

radiation angle at 30°. The measurement, performed with the fully expanded Mach 1.75 jet and repeated for many downstream locations of the OD sensor, results in a multitude of coherence plots that can be combined into the coherence contour plot, shown in Fig. 11. In this figure, the horizontal axis represents the downstream direction and the vertical axis the Strouhal number of the coherence. The vertical lines in the plot represent the downstream locations for which data were acquired. Locations in between are interpolated by the contour plot algorithm. The first observation one can make is that the maximum amount of coherence can be observed to be around 0.15, which demonstrates the moderately strong correlation between the flowfield and the acoustic far field. The region of maximum coherence is located within the first 6 diameters of the jet, which is consistent with the observations made from Fig. 10b, as well as with the noise source maps presented by McLaughlin et al. [25] with a Mach 1.5 jet. The coherence also peaks at a Strouhal number around 0.5 for the smallest downstream location ($3.6D$), with a very broad frequency peak. When going further downstream, the peak coherence shifts to lower Strouhal number and becomes narrower. This is consistent with the well-established scenario that the highest frequencies of the propagated noise are generated closer to the exit plane of the nozzle, where the turbulence has higher frequency content. Further downstream in the mixing layer, the turbulence grows and generates lower frequency noise. The coherence values decay to very low value past $13D$ downstream, which is consistent with the decrease in rms value observed from Fig. 6. This is also consistent with the coherence measurements made by Morrison and McLaughlin [26] in low Reynolds number supersonic jets. Finally, one can observe a drop of coherence around $7D$ downstream and a subsequent rise to another maximum further downstream, around $11D$. This was also visible in Fig. 10b and appears to be consistent with the noise source measurements made by Laufer et al. [22] in identifying two distinct regions of noise generation in supersonic jets. It is also noteworthy to mention that the end of the potential core of both the $M_j = 1.5$ and $M_j = 1.75$ jets are expected to be around $7D$ and $7.5D$, following observations from Lau et al. [27]. This corresponds to the dip in the correlation peak, pointing at the fact that the two distinct noise sources are located on either side of the end of the potential core.

All these results provide some further validation of the OD system and show that a significant amount of correlation, similar to what was obtained with the Rayleigh scattering technique by Panda and Seasholtz [11], can be obtained between flowfield measurements performed with the optical deflectometer and acoustic far-field measurements at the peak noise emission direction. The method can therefore potentially be used for noise source localization.

B. OD Sensors in the Near Field Correlated to Flowfield and Far-Field Measurements

While a significant amount of correlation was shown in the previous part between the flowfield and the acoustic far field, the OD measurements were confined to the jet flowfield. Since the OD technique relies on light refraction due to density gradients, it is possible for the system to provide some useful measurements outside of the jet, in the acoustic near field where strong pressure and density fluctuations still occur. Scanning of the near field was therefore attempted with OD sensors. The rms values of the optical signals were first determined and plotted against the radial location r/D, as shown in Fig. 12a for a fully expanded $M_j = 1.75$ jet. As expected, the strength of the signals drops significantly when the sensors exit the jet, reaching less than 3% of the peak value when $r/D > 1.0$. The same observation is true for all downstream locations, with slight changes in the rms values with downstream location. Moreover, the decay observed in the radial direction appears to follow an exponential curve. This is characteristic of a region of the near field where hydrodynamic pressure fluctuations are dominant. In this region, described in detail by Suzuki and Colonius [28], the pressure fluctuations contain components that do not propagate but rather decay exponentially with radial distance. Outside of this region, the rms of the OD sensor reaches a plateau value which is lower than the rms measured within the jet, but still above the noise floor (identified in Fig. 12a). In this region, the hydrodynamic pressure fluctuations have decayed to values lower than the propagating pressure waves, and the signals measured are therefore related to pressure fluctuations that propagate to the far field.

The spectral content of the signal can also be plotted for different radial distances from the jet centerline, as shown in Fig. 12b for $x/D = 5.5$. The magnitude of the power spectra decreases with radial location by several orders of magnitude, confirming the exponential decay observed from the rms plot. The shape of the spectra is also changing, with a much narrower peak at $r/D = 1.2$, which corresponds to the edge of the hydrodynamic fluctuation region. Further radially, the spectra flatten back but still remain above the noise floor. This shows an evolution of the physical phenomena being measured by the sensors, from hydrodynamic fluctuations to propagating acoustic waves further outward. It is also noteworthy to mention that since the spectra magnitudes are so low outside of the jet, measurements performed within the jet (and presented in the previous section) cannot be significantly contaminated due to integration effects through the acoustic field.

Since the jets being investigated are cold jets, the jet density is higher than the ambient density. This means there is a negative density gradient $\partial\rho/\partial r$ within the shear layer. In supersonically

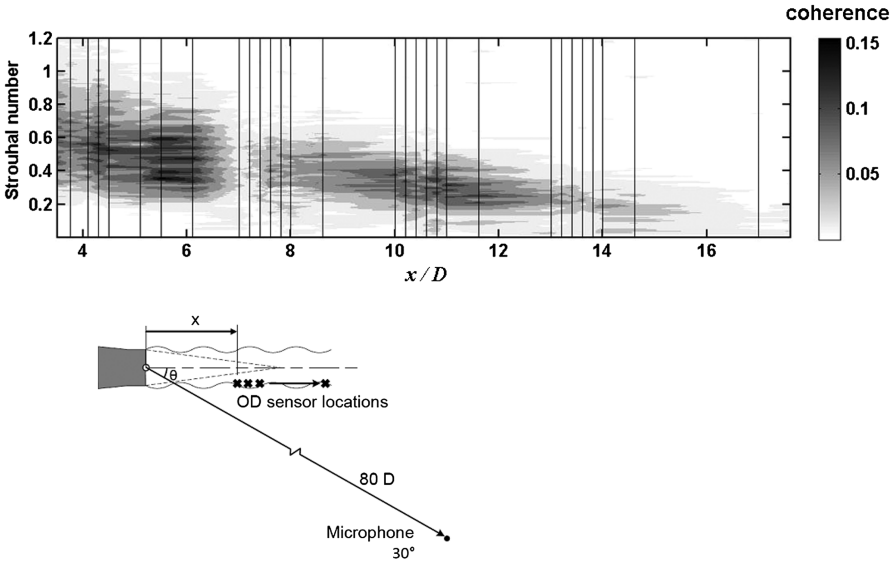

Fig. 11 Contour plots of the coherence between an OD sensor scanning along the lipline of a perfectly expanded $M_j = 1.75$ jet and a microphone fixed in the far field at $\theta = 30°$.

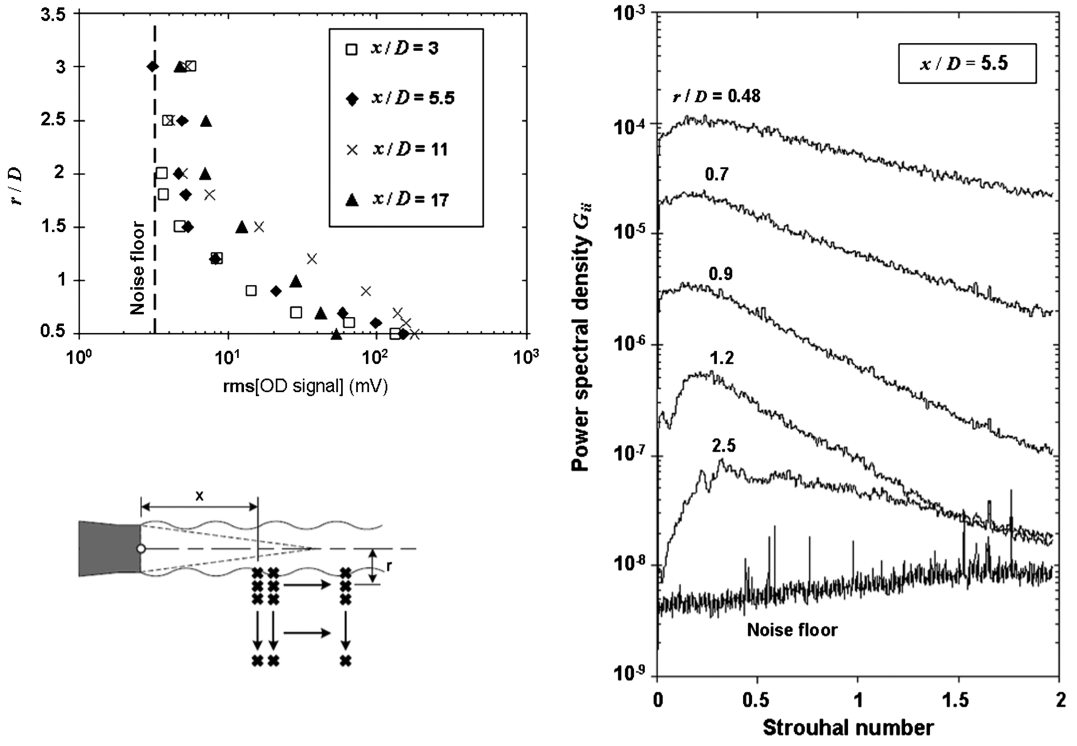

a) b)

Fig. 12 $M_d = M_j = 1.75$ jet: a) rms values of the optical signals at different axial locations x/D and radial positions r/D and b) power spectral density measured at different radial locations and at $x/D = 5.5$.

convecting jets, producing Mach wave radiation, there is also a sharp increase in density at one point in space outside of the jet, when a Mach wave propagates through this point. This also produces an instantaneous negative density gradient $\partial\rho/\partial r$. Therefore, on the light shear layer side of the jet, the wave front appears as a bright band, and on the dark shear layer side, as a dark band. This pattern can be observed in a fully expanded $M_d = M_j = 1.8$ jet on the spark Schlieren image presented in Fig. 13a. In such Schlieren visualization, dark and light shades of light represent regions of the flow with sharp density gradients of different directions. Arrows are placed at locations on Fig. 13a with strong instantaneous density gradients, with (the arrow) body going through the high density gradient region. Since the photodiodes used in the OD setup produce a decrease in voltage output for an increase of light intensity, the output voltage, once multiplied by -1, can be assumed to represent the fluctuations in density gradient. The skewness of that signal can therefore be calculated for different locations of the OD sensor signal outside of the jet and represent the skewness of the fluctuations of density gradient. Figure 13b presents the value of the skewness for the same jet condition and locations as the data from Fig. 12a. There is a large value of positive skewness close to the jet lip line, which grows for further downstream locations. In this region of high skewness, the sensors are still within the hydrodynamic region of the jet. For observations further outside the jet, in the region where the propagating acoustic waves dominate the signals, the skewness remains strongly positive. This is one of the first pieces of direct evidence that the strong skewness in the acoustic far field of high-speed jets (first identified by Ffowcs Williams et al. [29] and

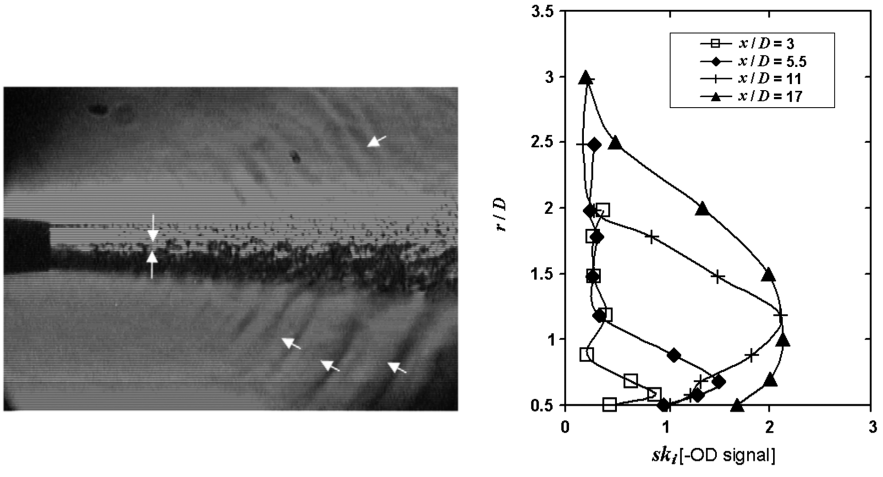

a) b)

Fig. 13 Optical measurements in a fully expanded $M_d = M_j = 1.8$ jet: a) spark Schlieren image (arrows located at regions with strong density gradient, pointing toward the high density) and b) skewness of the negative value of the signal from an OD sensor in the near field.

associated with the acoustic phenomenon known as "crackle") is also present in the hydrodynamic field and in the acoustic near field of the jet. This strongly supports the concept that crackle originates in the jet and is not a result (purely) of nonlinear distortion within the propagation region of the high amplitude noise.

The peaks of correlation can also be determined between optical sensors in the jet and ones that scan the near field. Figure 14 presents the value of the correlation between an optical sensor located at three downstream positions along the lipline of the jet and another optical sensor located at a downstream distance $\Delta x/D = 1$ from the first sensor and scanning the near field in the radial direction. There is obviously some high correlation for no radial displacement of the second sensor, since it measures the correlation of the flow structures convecting within the jet. With increasing values of $\Delta r/D$, the amount of correlation first drops as the sensor exits the jet but is still in the hydrodynamic region. Going further radially, the correlation increases again, reaching correlation peaks as high as 0.25. Since the sensor is now in the acoustic near field, this tends to show that this correlation corresponds to noise radiated by the structures passing through the location of the first sensor. With increasing axial location of the pair of sensors, this correlation peak flattens in the radial (r) direction and disappears all together for $x/D = 7$ and further downstream (measured up till $16D$). It therefore tends to show that the major noise production region within the mixing layer is confined to the first seven diameters downstream of the exit plane, which is consistent with the observations made from Figs. 10 and 11 and with observations made by Papamoschou et al. [17] from the same data but using a very different processing approach. The reader is reminded that this noise production region, shown for cold jets stretches well past 10 nozzle diameters for hot jets as shown in [25] among others.

Similarly to what was done with the optical measurements within the jet presented earlier, some knowledge can be gained regarding the frequency content that correlates with the acoustic far field by measuring the coherence rather than the cross-correlation coefficient function. This coherence is determined for two signals: 1) the OD sensor at a position just outside of the jet, at a constant downstream location and 2) the microphone located at $R/D = 80$ and $\theta = 30°$. The coherence values calculated for various OD sensor radial locations and downstream locations of $3D$, $6.1D$, $8D$ and $11D$ are assembled into contour plots shown in Fig. 15. The first observation to be made from these plots is that the coherence reaches very high values, with a maximum around 0.6, which means that the signals measured in the acoustic near field by the OD sensor are very strongly related to the far-field acoustic signal. This is noticeably higher than the coherence obtained between the acoustic far field and the OD measurements within the jet flow, which did not exceed 0.15. Furthermore, for different downstream locations of the OD sensor there is a very clear change in the radial position that gives the best correlation with the acoustic far field: the further downstream the sensors are positioned, the further radially the location of the peak of coherence appears. This trend seems to point to a localized region of the jet that produces the noise propagating in the peak emission direction ($\theta = 30°$). However, as shown by Bogey and Bailly [30] and pointed out by Papamoschou et al. [17], the ray connecting a point inside the jet to a point in the vicinity of the jet is not a straight line but rather is bent inside the jet due to refraction caused by velocity and sound speed gradients. It is therefore difficult to precisely localize the noise source from these measurements alone. The peak of coherence also occurs at a lower frequency when the optical sensors are located further from the jet. Finally, the radial region with maximum coherence widens at further downstream locations. Some of these effects may also have to do with the change in relative angle between the optical sensors and the microphones. Future experiments with a microphone fixed relative to the optical sensor location (rather than relative to the jet exit plane) would allow for some clarification of these data and an easier interpretation of the results.

To investigate the effect of the polar angle location of the far-field microphone on these correlations, the coherence can also be plotted as a function of θ. Figure 16a presents the coherence as a function of θ for an optical sensor fixed in the near field, at a radial and axial location corresponding to a peak of coherence as observed in Fig. 15 with respect to the microphone at $\theta = 30°$. The contour plot shows that the coherence is maximum around the $\theta = 30°$ direction and decreases to very low value for $\theta > 40°$. The near-field pressure fluctuations therefore seem to have a very strong directivity, around $\theta = 30°$. At this point, it should be noted that the jet considered is a fully expanded $M_j = 1.75$ jet, with a measured convection velocity that leads to a Mach wave radiation angle around $\theta = 30°$. A clear signature of the presence of crackle in the measured noise is the presence of a strong positive skewness [defined in Eq. (3)]. The value of the skewness as well as the overall sound pressure level (OASPL) are calculated for each far-field microphone and plotted in Fig. 16b. The skewness reaches a peak around 30 deg, while the OASPL is the highest for that same polar angle value. This concurs with the prediction of the Mach wave radiation angles as well as the peak coherence observed in Fig. 16a. Therefore, this constitutes proof that the signals measured by the OD sensors outside of the jet relate to the propagation of Mach waves that initially contain the characteristic of crackle and subsequently propagate to the far field. Careful measurements of this kind can therefore potentially give accurate localization and strength measurements of the Mach wave generation process as a function of downstream location.

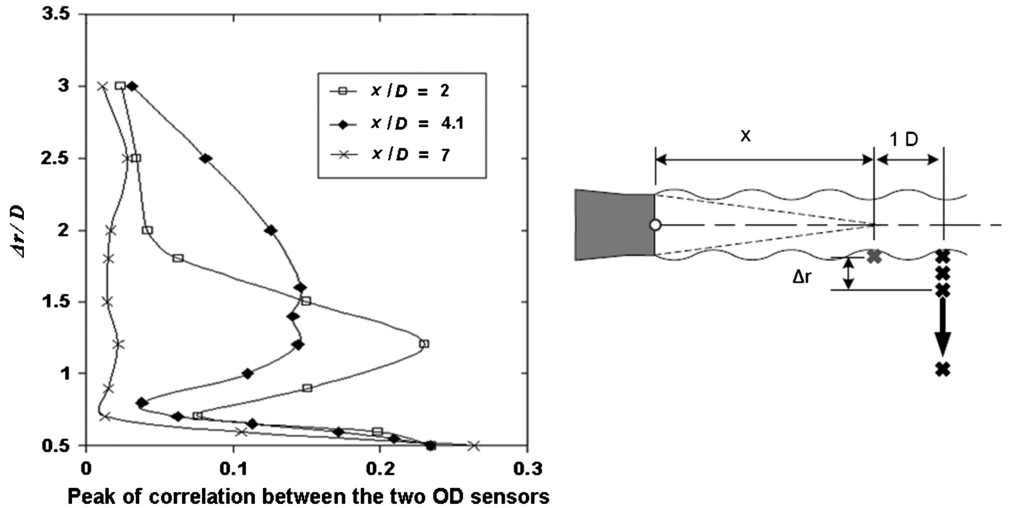

Fig. 14 Correlation peaks between one OD sensor at the lipline ($r = 0.5$) and different axial locations with an OD sensor scanning radially outward, 1 diameter further downstream ($\Delta x/D = 1$ and different values of $\Delta r/D$). $M_d = M_j = 1.75$.

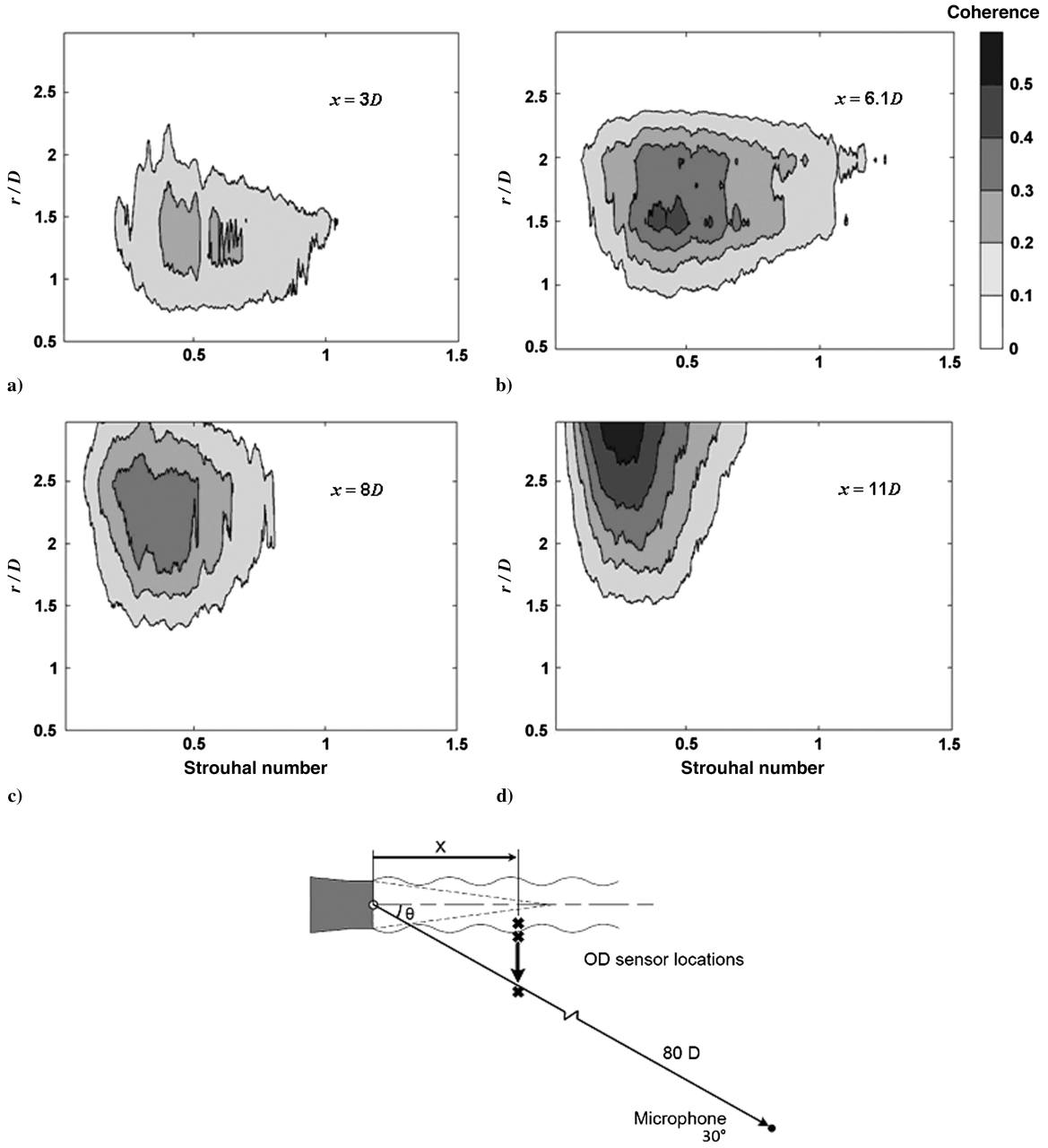

Fig. 15 Contour plots of the coherence between an OD sensor scanning outside the jet and microphone at 30° at different downstream locations: a) $x = 3D$, b) $x = 6.1D$, c) $x = 8D$, and d) $x = 11D$. $M_d = M_j = 1.75$.

C. OD Sensors in the Jet Correlated to Forward Arc Microphones

While the focus of the two previous parts was on the noise propagating to the peak noise direction, the acoustic spectra generated by shock-containing jets also contain a substantial amount of shock associated noise that is dominant in the forward arc. This noise component, called BBSAN, is created by the interaction of the shock cell structure of imperfectly balanced supersonic jets with the convecting turbulence. Therefore, some significant correlation should exist between the broadband turbulence within the jet and the BBSAN measured in the far field. To obtain some knowledge over the frequency range that correlates between the flowfield and the acoustic far-field measurements, one can look at the auto- and cross-spectra between an OD sensor and the signal from a microphone in the forward arc ($\theta = 97°$). As a representative example, Fig. 17 presents the auto- and cross-spectra as measured for a shock-containing jet $M_d = 1.0$, $M_j = 1.5$ jet with an optical sensor on the lip line at $x/D = 4.8$ and a microphone in the forward arc. The first observation one can make is that the largest spectral values are clearly in the very sharp peaks at $St = 0.28$, 0.32 and 0.56. These peaks are screech tones and have a relatively weak influence on the other components of the radiated noise when there is significant BBSAN [31]. Since screech is typically not observed in jets such as aircraft engine exhaust jets, little attention will be given to it in this study. The autospectrum of the signal from the OD sensor has a very broad peak around $St = 0.4$ and decreases slowly with increasing frequency. This is consistent with measurements performed by Panda and Seasholtz [11] with the Rayleigh scattering technique. On the other hand, the microphone signal has a peak at a frequency around $St = 0.5$, which corresponds to the BBSAN peak frequency for this specific polar angle. The resulting correlation between the two signals peaks at approximately the same frequency.

To look at this more closely, Figs. 18a and 18b present the coherence function between the OD sensor within the mixing layer and the far-field microphones in the forward arc, plotted together with the acoustic spectra. The resulting coherences and spectra are plotted for two $M_j = 1.8$ jets issuing from a purely converging $M_d = 1.0$ and from a converging-diverging $M_d = 1.5$ nozzle. These strongly underexpanded conditions produced no screech, as can be

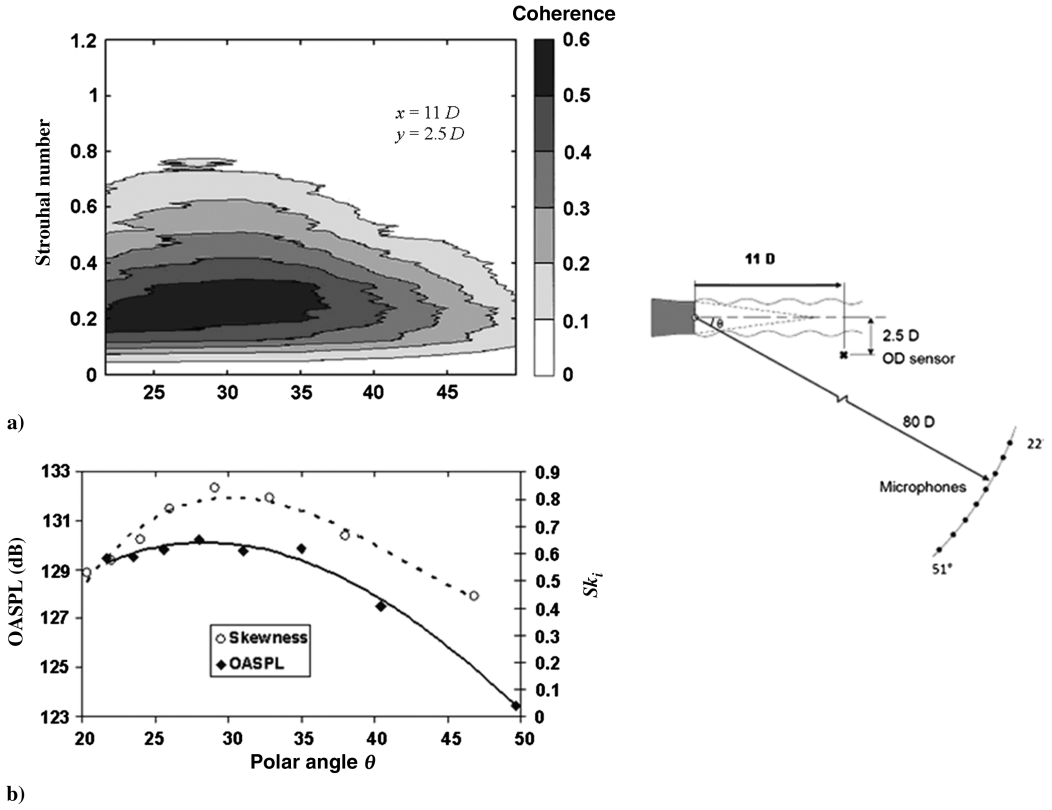

Fig. 16 Optical measurements in a fully expanded $M_d = M_j = 1.75$ jet at $x = 11D$ and $y = 2.5D$ and acoustic measurements at different polar angles in the rear arc: a) contour plots of the coherence between the OD sensor and the microphones and b) skewness and OASPL of the microphone signals.

seen on the acoustic spectra. The shock cell pattern from these nozzles can be seen in the Schlieren photographs of Figs. 18c and 18d, together with the location of the optical sensor within the jet. The schematic of the experiment is similar to the one from Fig. 17. A noteworthy observation is the presence of a Mach disk at the center of the most strongly underexpanded case jet, while the shock cell geometry for the $M_d = 1.5$ case looks more traditional, with a diamond shape shock cell structure. As a result, while both cases are strongly shock-containing, resulting in a large amount of BBSAN, the less imbalanced case is louder by about 5 dB at the peak across the presented range of polar angles. On the other hand, for both cases, there is a similar amount of coherence, as high as 0.04, between the OD sensor within the mixing layer and the far-field microphones. This is three times less than the observed maximum coherence with microphones in the rear arc. It is also very clear that the peak of coherence is at the same frequency as the peak in the BBSAN. Similar measurements performed with fully expanded (shock-free) jets exhibit no coherence at all (with microphones in the forward arc). This thus demonstrates some correlation between the convecting turbulent structures and the far-field BBSAN. Finally, as expected, when the polar angle shifts to higher values, the BBSAN shifts in frequency to lower values and the coherence follows the same trend. It therefore highlights the possibility to directly relate the flowfield fluctuations to the shock noise, dominant component of the noise in the forward arc for imperfectly balanced jets.

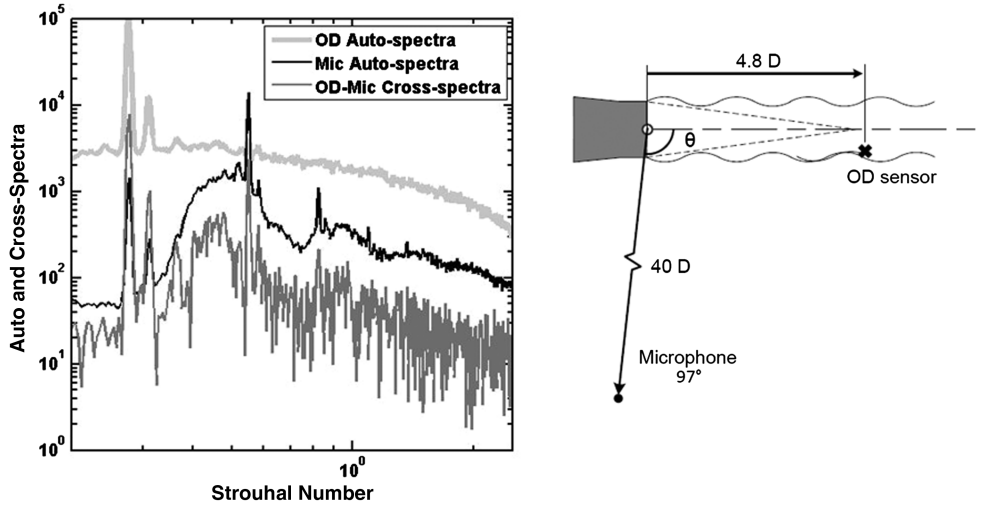

Fig. 17 Auto and cross spectra for a microphone at $\theta = 97°$ and an OD sensor on lipline at $x/D = 4.8$ in a $M_d = 1.0$, $M_j = 1.5$ shock-containing jet.

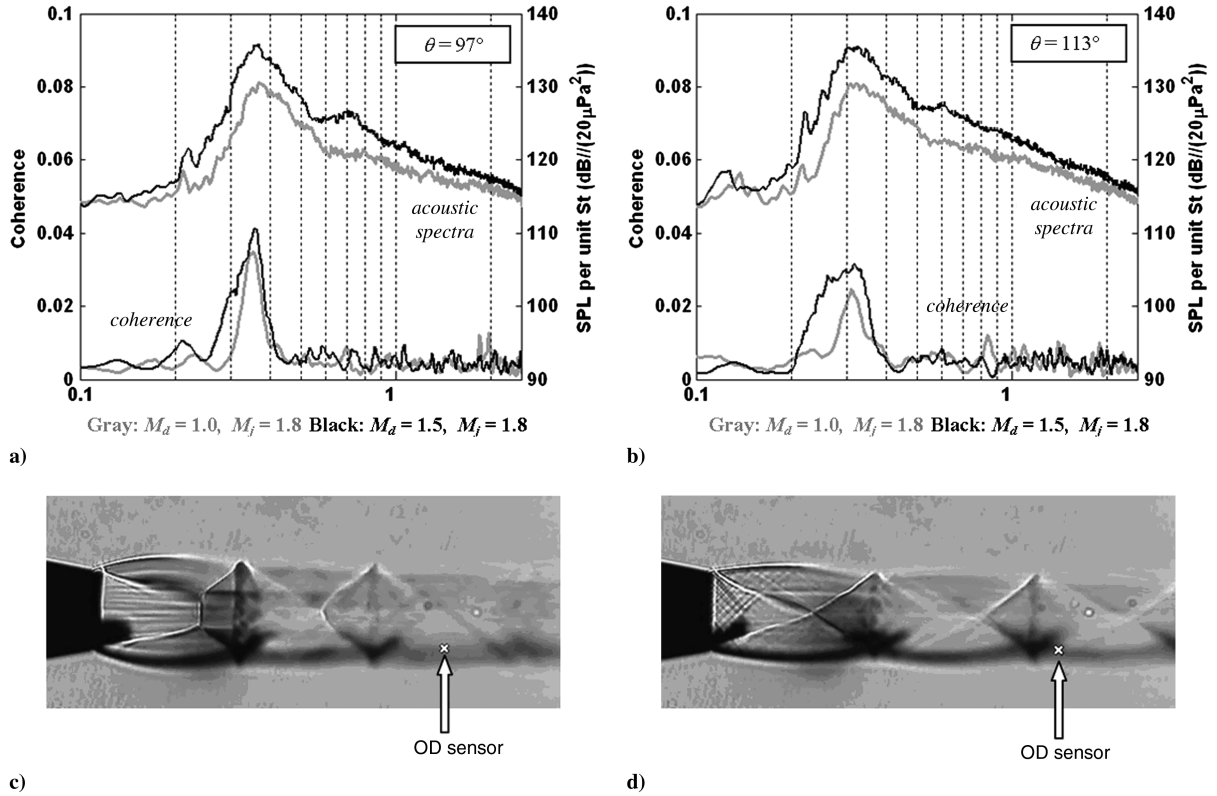

Fig. 18 Measurements in shock containing jets: a–b) far-field acoustic spectra and coherence between the microphones and OD sensors at the lip line, c) Schlieren image of the $M_d = 1.0, M_j = 1.8$ jet, and d) Schlieren image of the $M_d = 1.5, M_j = 1.8$ jet.

IV. Conclusions

A new OD system was developed and tested for the purpose of measurement of density gradient fluctuations within the jet, related to turbulence. The system was then used to produce direct correlation between the flowfield signals and those of the far-field microphones. Coherence as high as 0.15 was observed between sensors along the lipline and microphones in the peak noise emission direction. The optical sensors were then located outside of the jet, in an attempt to measure fluctuations in the acoustic near field. An exponential decay of the signal was observed, which is typical of hydrodynamic pressure fluctuations in the very near field. Further from the jet, the measured optical signals were shown to correlate more strongly with acoustic far-field measurements, with coherence peak values as high as 0.6. This demonstrates the ability of the technique to provide non intrusive measurements of the acoustic near field that could be used as a tool for noise localization or far-field noise prediction.

It is noted that the results contained in this paper have been obtained with jets operating at both $M_j = 1.5$ and $M_j = 1.75$, for which the turbulence (average) convective Mach numbers are subsonic and supersonic, respectively. Little evidence of any significant differences in the radiated noise and the correlation of that noise with the turbulence measurements was observed. This issue is the subject of further study in efforts to more fully understand the processed of high-speed jet noise.

While the OD technique is usually trusted only in pure air cold jet, such near-field measurements are possible with heated or heat-simulated jets and are particularly valuable with simultaneous acoustic far-field measurements. An initial significant result of such near-field measurements is the high level of skewness in these measurements that substantiate the concept that crackle observed in the far field, originates at the flowfield–acoustic-near-field interface. Finally, some additional measurements were performed with the OD sensors within the shear layer of the jet and the microphones in the forward arc of the plane with shock-containing jets. Significant coherence was observed between the flowfield measurements and the acoustic far field with peaks at the same frequency as the BBSAN. Once again, this shows the utility of the system in developing more understanding of the noise generation mechanisms.

Acknowledgments

This work was performed under the sponsorship of the NASA Research Agreement NNX08AAC44A monitored by James E. Bridges. The authors would like to acknowledge Dimitri Papamoschou and Philip J. Morris for their active collaboration with this project.

References

[1] Davies, P. O. A. L., Fisher, M. J., and Barratt, M. J., "The Characteristics of the Turbulence in the Mixing Region of a Round Jet," *Journal of Fluid Mechanics*, Vol. 15, No. 3, 1963, pp. 337–367. doi:10.1017/S0022112063000306

[2] Bradshaw, P., Ferriss, D. H., and Johnson, R. F., "Turbulence in the Noise-Producing Region of a Circular Jet," *Journal of Fluid Mechanics*, Vol. 19, No. 4, 1964, pp. 591–624. doi:10.1017/S0022112064000945

[3] Crow, S. C., and Champagne, F. H., "Orderly Structure in Jet Turbulence," *Journal of Fluid Mechanics*, Vol. 48, No. 3, 1971, pp. 547–591. doi:10.1017/S0022112071001745

[4] Morris, P. J., and Zaman, K. B. M. Q., "Velocity Measurements in Jets with Application to Noise Source Modeling," *Journal of Sound and Vibration*, Vol. 329, No. 4, 2010, pp. 394–414. doi:10.1016/j.jsv.2009.09.024

[5] McLaughlin, D. K., Morrison, G. L., and Troutt, T. R., "Experiments on the Instability Waves in a Supersonic Jet and Their Acoustic Radiation," *Journal of Fluid Mechanics*, Vol. 69, No. 1, 1975, pp. 73–85. doi:10.1017/S0022112075001322

[6] Troutt, T. R., and McLaughlin, D. K., "Experiments on the Flow and Acoustic Properties of a Moderate-Reynolds-Number Supersonic Jet," *Journal of Fluid Mechanics*, Vol. 116, No. 1, 1982, pp. 123–156. doi:10.1017/S0022112082000408

[7] Lau, J. C., "Laser Velocimeter Correlation Measurements in Subsonic and Supersonic Jets," *Journal of Sound and Vibration*, Vol. 70, No. 1,

1980, pp. 85–101.
doi:10.1016/0022-460X(80)90556-8
[8] Kerhervé, F., Jordan, P., Gervais, Y., Valiere, J.-C., and Braud, P., "Two-Point Laser Doppler Velocimetry Measurements in a Mach 1.2 Cold Supersonic Jet for Statistical Aeroacoustic Source Model," *Experiments in Fluids*, Vol. 37, No. 2, 2004, pp. 419–437.
[9] Bridges, J., "Effect of Heat on Space-Time Correlations in Jets," AIAA Paper 2006-2534-924, 2006.
[10] Kastner, J., Kim, J. H., and Samimy, M., "Correlation of Large Scale Structure Dynamics and Far-Field Radiated Noise in a Mach 0.9 Jet," AIAA Paper 2007-830, 2007.
[11] Panda, J., and Seasholtz, R. G., "Experimental Investigation of Density Fluctuations in High-Speed Jets and Correlation with Generated Noise," *Journal of Fluid Mechanics*, Vol. 450, No. 1, 2002, pp. 97–130.
doi:10.1017/S002211200100622X
[12] Panda, J., Seasholtz, R. G., and Elam, K. A., "Investigation of Noise Sources in High-Speed Jets via Correlation Measurements," *Journal of Fluid Mechanics*, Vol. 537, No. 1, 2005, pp. 349–385.
doi:10.1017/S0022112005005148
[13] Doty, M. J., and McLaughlin, D. K., "Space-Time Correlation Measurements of High-Speed Axisymmetric Jets Using Optical Deflectometry," *Experiments in Fluids*, Vol. 38, No. 4, 2005, pp. 415–425.
doi:10.1007/s00348-004-0920-1
[14] Harper-Bourne, M., and Fisher, M. J., "The Noise from Shock-Waves in Supersonic Jets," AGARD CP-131, 1973, pp. 1–13.
[15] Seiner, J. M., and Reethof, G., "On the Distribution of Source Coherency in Subsonic Jets," AIAA Paper No. 74-4, 1974.
[16] Schaffar, M., "Direct Measurements of the Correlation Between Axial In-Jet Velocity Fluctuations and Far-Field Noise Near the Axis of a Cold Jet," *Journal of Sound and Vibration*, Vol. 64, No. 1, 1979, pp. 73–83.
doi:10.1016/0022-460X(79)90573-X
[17] Papamoschou, D., Morris, P. J., and McLaughlin, D. K., "Beamformed Flow-Acoustic Correlations in High-Speed Jets," AIAA Paper 2009-3212, 2009.
[18] Doty, M. J., and McLaughlin, D. K., "Acoustic and Mean Flow Measurements of High Speed Helium Air Mixture Jets," *International Journal of Aeroacoustics*, Vol. 2, Nos. 3–4, 2003, pp. 293–334.
doi:10.1260/147547203322986151
[19] McLaughlin, D. K., Bridges, J., and Kuo, C.-W., "On the Scaling of Small, Heat Simulated Jet Noise Measurements to Moderate Size Exhaust Jets," *International Journal of Aeroacoustics*, Vol. 9, Nos. 4–5, 2010, pp. 627–654.
doi:10.1260/1475-472X.9.4-5.627
[20] Harper-Bourne, M., "Jet Noise Turbulence Measurements," AIAA Paper No. 2003-3214, 2003.
[21] Kerhervé, F., Fitzpatrick, J., and Jordan, P., "The Frequency Dependence of Jet Turbulence for Noise Source Modeling," *Journal of Sound and Vibration*, Vol. 296, Nos. 1–2, 2006, pp. 209–225.
doi:10.1016/j.jsv.2006.02.012
[22] Laufer, J., Schlinker, R. H., and Kaplan, R. E., "Experiments on Supersonic Jet Noise," *AIAA Journal*, Vol. 14, No. 4, 1976, pp. 489–497.
[23] Seiner, J. M., McLaughlin, D. K., and Liu, C. H., "Supersonic Jet Noise Generated by Large-Scale Instabilities," NASA TP 2072, Sept. 1982.
[24] Day, B. J., "Turbulence Measurements in Supersonic Jets with Optical Deflectometry," M.S. Thesis, Pennsylvania State Univ., University Park, PA, May 2010.
[25] McLaughlin, D. K., Kuo, C. W., and Papamoschou, D., "Experiments on the Effect of Ground Reflections on Supersonic Jet Noise," AIAA Paper 2008-22, 2008.
[26] Morrison, G. L., and McLaughlin, D. K., "Noise Generation by Instabilities in Low Reynolds Number Supersonic Jets," *Journal of Sound and Vibration*, Vol. 65, No. 2, 1979, pp. 177–191.
doi:10.1016/0022-460X(79)90512-1
[27] Lau, J. C., Morris, P. J., and Fisher, M. J., "Measurements in Subsonic and Supersonic Free Jets Using a Laser Velocimeter," *Journal of Fluid Mechanics*, Vol. 93, No. 1, 1979, pp. 1–27.
doi:10.1017/S0022112079001750
[28] Suzuki, T., and Colonius, T., "Instability Waves in a Subsonic Round Jet Detected Using a Near-Field Phased Microphone Array," *Journal of Fluid Mechanics*, Vol. 565, No. 1, 2006, pp. 197–226.
doi:10.1017/S0022112006001613
[29] Ffowcs Williams, J. E., Simson, J., and Virchis, V. J., "'Crackle': An Annoying Component of Jet Noise," *Journal of Fluid Mechanics*, Vol. 71, No. 2, 1975, pp. 251–271.
doi:10.1017/S0022112075002558
[30] Bogey, C., and Bailly, C., "An Analysis of the Correlations Between the Turbulent Flow and the Sound Pressure Fields of Subsonic Jets," *Journal of Fluid Mechanics*, Vol. 583, 2007, pp. 71–97.
doi:10.1017/S002211200700612X
[31] Veltin, J., and McLaughlin, D. K., "Noise Mechanisms Investigation in Shock Containing Screeching Jets Using OD," AIAA Paper 2008-288, 2008.

E. Gutmark
Associate Editor